

## Chain Growth Reactions of Methanol on SAPO-34 and H-ZSM5

Enrique Iglesia, Tom Wang, and Sara Y. Yu

Department of Chemical Engineering, University of California at Berkeley, Berkeley CA 94720

### ABSTRACT

Reactions of  $C_3H_6/^{13}CH_3OH$  mixtures show that chains grow via methylation of adsorbed intermediates with  $CH_3OH$  on H-ZSM5 and SAPO-34 and alkenes desorb via  $\beta$ -scission steps. Turnover rates are faster on H-ZSM5 than on SAPO-34 and they increase with residence time and with the addition of alkenes on H-ZSM5, because  $\beta$ -scission rates are higher for the larger growing chains favored at such conditions. Rates do not increase with alkene concentration on SAPO-34 because transport processes control the rate at which alkenes enter the gas phase. Ethene is a minor product on H-ZSM5 because  $\beta$ -scission pathways favor the formation of  $C_3^+$  products. The lower turnover rates, faster deactivation, and higher ethene selectivities on SAPO-34 reflect diffusional constraints imposed by the small connections between intracrystalline cavities. Light alkenes are selectively extracted from equilibrated alkene mixtures formed within elliptical cavities in SAPO-34. The reactivity of alkenes of varying length and structure during  $^{13}CH_3OH$  reactions confirms these conclusions. Intermediate transport restrictions lead to maximum ethene selectivities and appear to require small SAPO-34 crystals with few external acid sites.

### 1. INTRODUCTION

Medium-pore pentasil zeolites (H-ZSM5) with low Al content [1] and small crystallites of SAPO-34, a silicoaluminophosphate with chabazite structure [2], are effective in methanol conversion to light alkenes [3,4]. SAPO-34 shows higher selectivity to ethylene, but it deactivates rapidly and requires frequent regeneration [5]. Several reactive intermediates (carbenes, oxonium ylides, radicals, oxoniums) have been proposed for initial C-C bond formation steps on H-ZSM5 [6]. Some reports conclude that ethylene is the first alkene product [7-9], but others favor the initial desorption of larger alkenes [10-12]. On small-pore SAPO-34, the slow diffusion of products can lead to selective sieving of smaller ethene products from a complex mixture of alkenes [13]. Extracrystal acid sites and transport restrictions can obscure mechanistic details on SAPO-34, but recent  $C_2H_5OH-^{13}CH_3OH$  co-feed studies suggest that light alkenes can form via  $\beta$ -scission of larger alkenes [14,15].

In this study, reaction pathways required for methanol conversion to light alkenes on H-ZSM5 and SAPO-34 are probed using kinetic and isotopic tracer methods at conditions leading to high  $C_2$ - $C_5$  alkene selectivity ( $> 70\%$ ). Our data show that methylation and  $\beta$ -scission of large carbocations leads to the formation of alkenes. Ethene formation is not favored by these  $\beta$ -scission steps; ethene selectivity increases as methylation/ $\beta$ -scission steps approach equilibrium at long bed or intraparticle residence times.

### 2. METHODS

H-ZSM-5 was obtained by  $NH_4NO_3$  exchange of Na-ZSM-5 (Si/Al=175; 0.5, 1, 2, and 4  $\mu$  average crystal diameter) [16] and treatment in dry air at 773 K. The Al content is 0.096 mmol/g (2  $\mu$  sample); it agrees well with the number of  $NH_3$  desorbed during decomposition of exchanged  $NH_4^+$  (0.11 mmol/g) and corresponds to a  $H^+$  density of 0.55  $H^+/u.c.$  (0.11  $H^+/nm^3$ ). A sample with Si/Al ratio of 14.5 (Zeochem) was exchanged using the same procedure [17].

SAPO-34 was prepared by the procedure of reference [2]. The Si content was 1.15 mmol/g and the  $\text{NH}_3$  uptake was 1.03 mmol/g ( $\text{H}^+$  density: 2.5  $\text{H}^+/\text{u.c.}$ , 1.0  $\text{H}^+/\text{nm}^3$ ). Scanning electron microscopy showed cubic crystallites of 0.3 to 0.7  $\mu$  diameter. X-ray diffraction and electron micrographs showed that H-ZSM5 and SAPO-34 samples had excellent crystallinity.

Methanol reactions were carried out in a gradientless batch reactor [17] on H-ZSM5 (673 K, 11-12 mg) and SAPO-34 (653 K, 5-6 mg) at conversions per pass below 2-3%. Samples were treated in air at 823 K for 1 h before reaction. He (85 kPa, >99.95%) and  $\text{H}_2\text{O}$  (5 kPa) were used to dilute  $\text{CH}_3\text{OH}$  (10 kPa, Fisher Certified).  $\text{C}_2\text{H}_4$ ,  $\text{C}_3\text{H}_6$ , 1- $\text{C}_4\text{H}_8$ , and iso- $\text{C}_4\text{H}_8$  (1 kPa, C.P., >99.5%) were mixed with  $^{13}\text{C}_3\text{H}_7\text{OH}$  (10 kPa, 99%  $^{13}\text{C}$ , Cambridge Isotopes) in co-feed studies. Chemical and isotopic contents were measured by chromatography using flame ionization and mass selective detection. Isotomer distributions were obtained from mass fragmentation data [18].

### 3. RESULTS AND DISCUSSION

Selectivities and methanol conversion rates per acid site are shown in the Table on H-ZSM5 and SAPO-34 at similar reactant ( $\text{CH}_3\text{OH} + \text{CH}_3\text{OCH}_3$ ) conversion. SAPO-34 gives lower turnover rates and  $\text{C}_6+$  selectivity than H-ZSM5 and much higher ethene/propene ratios. Alkene/alkane ratios are very high (>10) on both samples at all conversions. Turnover rates are initially low on H-ZSM5, but reach the values in the Table as conversion increases with increasing contact time (Figure 1). No initial induction was observed on SAPO-34 (Figure 1).

Table. Methanol conversion to light alkenes on H-ZSM5 (Si/Al=175) and SAPO-34 [673K, 10kPa  $\text{CH}_3\text{OH}$ , 5 kPa  $\text{H}_2\text{O}$ , 38.5-39% methanol/DME conversion]

	H-ZSM5	SAPO-34
Site Density (mmol/g)	0.096	1.15
Turnover Rate ( $\text{s}^{-1}$ )	0.64	0.15
Selectivity (C%)		
C <sub>1</sub>	0.44	0.70
C <sub>2</sub>	1.4	29.1
C <sub>3</sub>	34.5	48.1
C <sub>4</sub>	22.6	16.5
C <sub>5</sub> (iso/normal ratio)	13 (0.74)	4.2 (0.09)
C <sub>6+</sub>	26.8	1.1
Ethene/Ethane	75	238
Propene/Propane	370	13

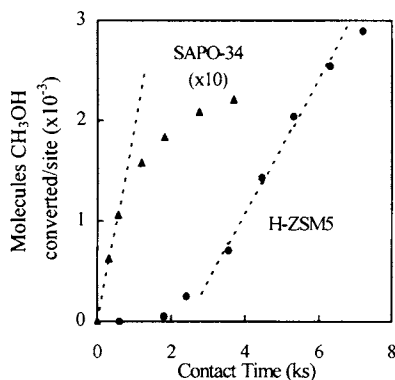


Figure 1.  $\text{CH}_3\text{OH}$  conversion turnovers on H-ZSM5 and SAPO-34 (x10) in gradientless batch reactor [673 K, 10 kPa  $\text{CH}_3\text{OH}$ , 5 kPa  $\text{H}_2\text{O}$ ]

The evolution of products with contact time resembles that reported by others [1].  $\text{CH}_3\text{OH}$ - $\text{CH}_3\text{OCH}_3$  equilibrium is fast, alkene selectivities reach a maximum at intermediate conversions, and aromatics and larger alkanes become more abundant as contact time increases. These trends are similar on SAPO-34 and H-ZSM5, but ethene and  $\text{C}_6+$  selectivities differ on the two catalysts. The effect of conversion on  $\text{C}_2\text{H}_4/\text{C}_3\text{H}_6$  ratios is shown in Figure 2. On SAPO-34, ethene selectivity increases slightly as conversion increases; ethene becomes a

favored product only as alkenes approach equilibrium at long contact times. On H-ZSM5 (2  $\mu$ , Si/Al=175),  $C_2H_4/C_3H_6$  ratios are much smaller and increase slightly with contact time, except at very low conversions, where this ratio is very high and decreases sharply with increasing contact time. These high initial ethene selectivities have been misinterpreted as evidence for ethene as the initial alkene formed in methanol reactions.

Ethene/propene ratios on H-ZSM5 did not depend on crystal size for samples with low Al content, but reached higher values on Al-rich H-ZSM5 (Figure 3). The x-axis in Figure 3 [the product of  $L^2$  ( $L$ , crystal diameter) and acid sites per unit volume] consists of a Thiele parameter that reflects the severity of intracrystal transport restrictions. The higher  $C_2H_4/C_3H_6$  ratios obtained at high values of this parameter reflect the intracrystalline equilibration of alkene mixtures as intracrystal residence time increases with increasing severity of transport restrictions. Ethene is abundant in equilibrated alkene mixtures, but  $\beta$ -scission kinetics favor the desorption of  $C_3+$  alkenes. High ethene selectivities on SAPO-34 reflect diffusional restrictions that become more severe for larger alkenes and lead to equilibrated alkene mixtures within SAPO-34 cavities.

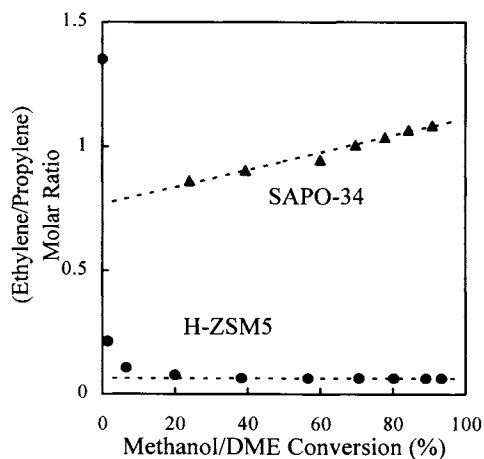


Figure 2. Ethene/Propene ratio in reaction products [673 K, 10kPa  $CH_3OH$ , 5 kPa  $H_2O$ ]

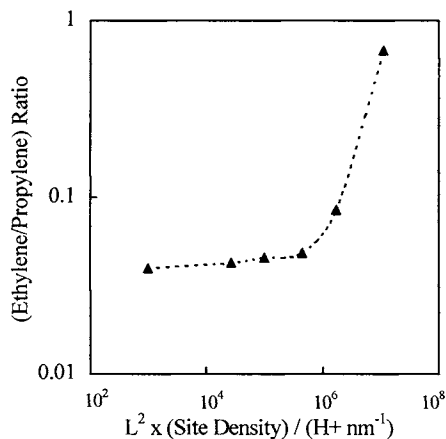
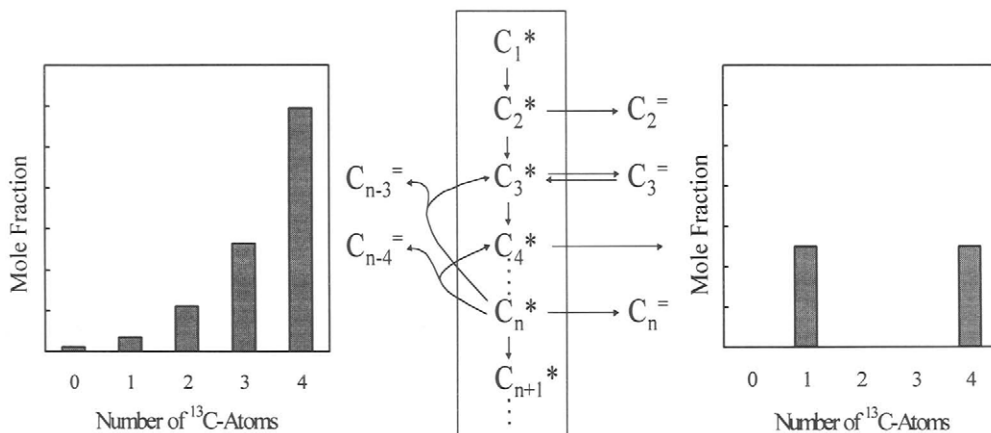


Figure 3. Effect of transport restrictions  $\{L^2 \times (\text{site density})\}$  on ethene/propene ratio [673K, 10 kPa  $CH_3OH$ , 5 kPa  $H_2O$ , 45-55% methanol/dimethyl-ether conversion]

Chain growth pathways were probed using  $C_3H_6/^{13}CH_3OH$  reactant mixtures. The Scheme shows two chain growth paths and the isotopomer distributions expected for butenes formed via each path. Chains growing by methylation of carbocations can terminate as alkenes by deprotonation or by  $\beta$ -scission chain transfer steps. The latter path preserves a smaller carbocation and avoids the need to re-form chains from methanol after each turnover.  $\beta$ -Scission from intermediates that undergo fast isomerization and intramolecular scrambling of carbons (from  $C_3H_6$  or  $^{13}CH_3OH$ ) would lead to binomial isotopomer distributions. Deprotonation removes an intact chain, which can only form from a specific number of  $C_3H_6$  or  $^{13}CH_3OH$  molecules. Thus, butenes can only contain either four  $^{13}C$  atoms (from  $^{13}CH_3OH$ ) or one  $^{13}C$  (from one  $^{13}CH_3OH$  and one  $C_3H_6$ ).



Scheme. Chain growth pathways and expected isotopomer distributions in butene formed from  $C_3H_6/^{13}CH_3OH$  mixtures

$C_3H_6/^{13}CH_3OH$  reactants lead to binomial isotopomer distributions in all  $C_4$  olefins (Figure 4) on H-ZSM5 (Si/Al=175), except at the low conversions within initial induction periods, suggesting that products form by sequential methylation and  $\beta$ -scission of large carbocations. Turnover rates, selectivities, and isotopomer distributions were not affected by crystal size on H-ZSM5 (Si/Al=175) or by contact time (after the initial induction period), confirming that these data reflect primary chain growth pathways, uncorrupted by intracrystalline transport restrictions and secondary reactions within channels. The hexene fraction contains only molecules with three or more  $^{13}C$  atoms; thus, alkene oligomerization does not occur during methanol conversion on kinetic-limited H-ZSM5 catalysts.

These methylation-cracking pathways avoid the need for the chain initiation from  $CH_3OH$  after each alkene formation turnover, but they lead to low ethene selectivity, because of the low ethene selectivity of  $\beta$ -scission pathways, and to an increase in reaction rate as the average growing chain becomes larger with increasing alkene concentration. These “living” intermediates form as small chains hydrogen transfer steps that also form methane and ethane, the most abundant products along with ethene during the initial induction period. At low conversions, chains are small because alkenes are unavailable to readsorb and maintain long chains at steady-state. Thus, termination occurs predominantly by deprotonation at low conversions and reaction rates are slow because chains must be initiated using  $CH_3OH$ - $CH_3OCH_3$  equilibrated mixtures after each turnover. The isotopomer distribution in 1-butene formed from  $C_3H_6/^{13}CH_3OH$  mixtures at low conversions (Figure 4) contains a larger than statistical concentration of butenes with one  $^{13}C$ , which can only form by the intact desorption of butyl cations formed from one  $C_3H_6$  and one  $^{13}CH_3OH$ .

Binomial isotopomer distributions were also obtained from alkene- $^{13}CH_3OH$  reactants on SAPO-34, but their assignment to methylation-cracking pathways is difficult, because transport restrictions and secondary reactions are not negligible on these small-pore catalysts. Added alkenes are less reactive on SAPO-34 than on H-ZSM5, because they diffuse through intercavity ports with much greater difficulty than methanol. Products form preferentially from the faster diffusing  $^{13}CH_3OH$  molecules in the reactant mixture.  $C_3H_6/^{13}CH_3OH$  gives a higher than statistical fraction of singly labeled 1- $C_4H_8$ . This isotopomer becomes more abundant on less crystalline SAPO-34 samples, suggesting that it forms via parallel pathways on

extracrystalline weak acid sites. These sites are less reactive but more accessible to added alkenes than intracrystalline acid sites.

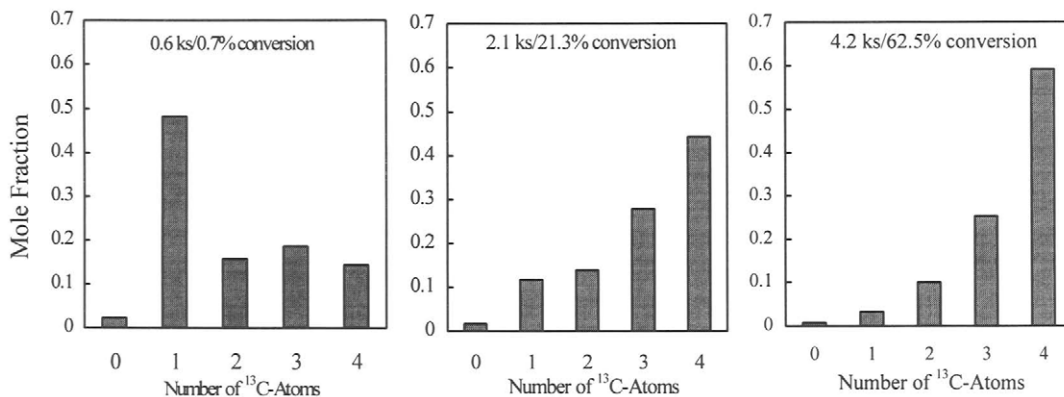


Figure 4. Isotopomer distribution in the butene products of  $C_3H_6/^{13}CH_3OH$  reactant mixtures (legend: contact time/methanol+DME conversion) [H-ZSM5, Si/Al=175, 2  $\mu$ , 673 K, 10 kPa  $CH_3OH$ , 5 kPa  $H_2O$ ]

The  $^{12}C$ -content in  $C_{n+1}$  alkenes formed from  $C_nH_{2n}/^{13}CH_3OH$  reactants reflects the relative reactivity of methanol and  $C_n$  alkenes. The  $^{12}C$  content in products is much higher on H-ZSM5 than on SAPO-34, even though reactions occur via carbocation pathways on both catalysts, because transport restrictions limit the availability of added alkenes for chain growth. The reactivity of alkenes increases with chain length on H-ZSM5 (Fig. 5), as expected in acid-catalyzed pathways. The opposite trend, however, is observed on SAPO-34 (Fig. 5). Reactivity differences between H-ZSM5 and SAPO-34 become greater for larger alkenes. These differences reflect the effectiveness factor for alkene reactions on diffusion-limited SAPO-34. Isobutene is less reactive than n-butene on SAPO-34, even though the kinetics of alkene reactions on acid sites favor branched alkenes (as observed on H-ZSM5). Alkenes formed from  $CH_3OH$  within SAPO-34 cavities must also overcome these diffusional constraints as they exit the crystals. Lower alkenes are consequently sieved by SAPO-34 crystals, but larger or branched alkenes remain and approach methylation/ $\beta$ -scission and isomerization equilibrium, in agreement with in-situ NMR studies [13]. Isopentane to n-pentane ratios in products of  $CH_3OH$  reactions are near equilibrium on H-ZSM5 (0.74, Table), but very low (0.09) on SAPO-34, because of the selective sieving of linear chains over branched products by the small apertures in SAPO-34. The sieving of alkenes from equilibrated mixtures leads to high selectivity to ethene, a minority product of  $\beta$ -scission kinetics, and to low selectivity to branched alkenes on SAPO-34 but not on H-ZSM5. Such transport restrictions may also lead to the lower methanol turnover rates measured on SAPO-34 (Table). Low initial rates are not observed on SAPO-34 (Figure 1), because reaction rates are not limited by the kinetics of  $\beta$ -scission, but by transport rates.

Sieving from equilibrated methanol-alkene mixtures leads to product selectivities that depend on the relative diffusivity of alkenes through intercavity apertures in SAPO-34 (0.43 nm). The average chain length within this equilibrated mixture, however, depends on the relative diffusivities of methanol reactants and alkenes because the effective pressure of alkenes

within SAPO-34 cavities (0.67 x 1.01 nm) increases with increasing diffusion pathlength (crystal size) and methanol reaction rates (acid site density). Severe diffusional restrictions lead to sieving of light alkenes, but from mixtures of larger alkenes and with significantly greater propensity for unreactive polymeric residues. Kinetically-limited small SAPO-34 crystals (or H-ZSM5 crystals with channels larger than SAPO-34) lead to poor sieving and to the formation of the  $C_3+$  alkenes favored by primary  $\beta$ -scission pathways. Optimum ethylene selectivities appear to require intermediate levels of transport restrictions, while higher stability requires unencumbered transport. An optimum compromise appears to be reached on relative small (<0.5  $\mu$ ) SAPO-34 crystals [3]. H-ZSM5 (0.51-0.56 channel diameter), while more stable, does not provide any sieving selectivity for alkenes during methanol conversion, because the kinetic diameters of linear  $C_2$ - $C_4$  hydrocarbons (0.4-0.5 nm) are smaller than the channel dimensions in H-ZSM5, but similar in size to the intercavity ports in SAPO-34.

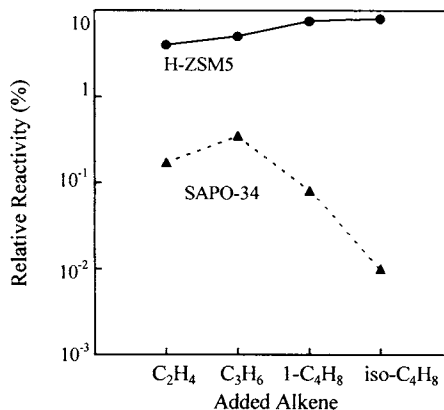


Figure 5. Relative alkene/methanol reactivity (mole basis) obtained from the isotopic content of the  $C_{n+1}$  alkene products of  $^{12}C_nH_{2n}/^{13}CH_3OH$  mixtures [673 K, 10kPa  $^{13}CH_3OH$ , 0.96 kPa  $^{12}C_nH_{2n}$ , 5 kPa  $H_2O$ ]

## REFERENCES

- [1] C.D. Chang, *Catal. Rev. Sci. Eng.* 26 (1984) 233.
- [2] B.M. Lok, C.A. Messina, R.L. Patton, R.T. Gajek, T.R. Cannan, E.M. Flannigen, *J. Am. Chem. Soc.* 106 (1984) 6092; U.S. Patent 4 440 871.
- [3] S.W. Kaiser, *Arab. J. Sci. Eng.* 10 (1985) 361; P.T. Barger, S.T. Wilson, J.S. Holmgren, U.S. Patent 5 126 308 (1982).
- [4] A.J. Marchi, G.F. Froment, *Appl. Catal.* 71 (1991) 139.
- [5] B.V. Bora, T.L. Marker, P.T. Barger, H.R. Nilsen, S. Kvisle, *Stud. Surface Sci. Catal.* 107 (1997) 87.
- [6] G.J. Hutchings, R. Hunter, *Catal. Today* 6 (1990) 279.
- [7] W.W. Kaeding, S.A. Butter, *J. Catal.* 61 (1980) 155.
- [8] W.O. Haag, R.M. Lago, P.G. Rodenwald, *J. Mol. Catal.* 17 (1982) 161.
- [9] M.M. Wu, W.W. Kaeding, *J. Catal.* 88 (1984) 478.
- [10] R.M. Dessau, R.B. LaPierre, *J. Catal.* 78 (1982) 136.
- [11] R.M. Dessau, *J. Catal.* 99 (1986) 111.
- [12] B. Sulikowski, J. Klinowski, *Appl. Catal.* 89 (1992) 69.
- [13] M.W. Anderson, B. Sulikowski, P.J. Barrie, J. Klinowski, *J. Phys. Chem.* 94 (1990) 2730.
- [14] I.M. Dahl, S. Kolboe, *Catal. Lett.* 20 (1993) 329.
- [15] I.M. Dahl, S. Kolboe, *J. Catal.* 149 (1994) 458.
- [16] J.P. Verduijn, *Intern. Pat. WO 93/08124* (1993).
- [17] J.A. Biscardi, E. Iglesia, *Catal. Today* 31 (1996) 207.
- [18] G.L. Price and E. Iglesia, *Ind. Eng. Chem. Res.* 28 (1989) 839.